

Enable Batteryless Flex-sensors via RFID Tags

Mengning Li

Department of Electrical and Computer Engineering

NC State University

Raleigh, USA

mli55@ncsu.edu

Abstract—Flex-angle detection of objects or human bodies has potential applications in robotic arm control, medical rehabilitation, and deformation detection. However, current solutions such as flex sensors and computer vision methods have limitations, such as the limited system lifetime of battery-powered flex sensors and the failure of computer vision methods in Non-Line-of-Sight (NLoS) scenarios. To overcome these limitations, we propose an RFID-based flex-sensor system, called RFlexor, which enables batteryless flex-angle detection in NLoS scenarios. RFlexor utilizes the change in tag phase and Received Signal Strength Indicator (RSSI) caused by the flexing of the tag to detect flex-angles. To extract the complex relationship between tag phase/RSSI and flex-angle, we train a multi-input AI model. We address the significant technical challenges by reformulating the phase and RSSI models, using phase difference and RSSI ratio as inputs, and applying multi-head attention to fuse phase and RSSI data. We implement the RFlexor system using Commercial-Off-The-Shelf (COTS) RFID devices and conduct extensive experiments. The results show that RFlexor achieves fine-grained flex-angle detection with a detection error of fewer than 10 degrees and a probability higher than 90% in most conditions. The average detection error is always less than 10 degrees across all experiments. Overall, RFlexor provides a promising solution for flex-angle detection in various scenarios.

Index Terms—RFID, Flex-angle Detection, Batteryless

I. INTRODUCTION

A. Motivation and Problem Statement

In the era of Internet-of-Things (IoT), detecting flex-angles of objects or human bodies (*e.g.*, fingers and arms) can benefit various application scenarios. For example, in smart manufacturing scenarios, the grasping state of a robotic arm can be monitored by measuring its flex-angle. In medical rehabilitation scenarios, doctors can diagnose the degree of a patient’s recovery by monitoring the flex angles of their joints. In mixed reality application scenarios, the detected flex-angles of objects can be used to check if the surface is flat or damaged, coming with a more immersive interactive experience. Generally, there are two types of solutions, including flex sensor [1], [2] and computer vision [3] methods, to the flex-angle detection problem. However, they have the following limitations: (i) flex sensors require batteries to power up, which inevitably limits the system lifetime; (ii) computer vision methods have strong requirements on Line-of-Sight (LoS). To overcome the limitations of the existing solutions, we for the first time study how to enable batteryless flex-sensors via Commercial-Off-The-Shelf (COTS) RFID tags.

As illustrated in Fig. 1, we describe the tag flex-angle detection problem in detail. Specifically, Fig. 1(a) shows a

3D schematic diagram, where the tag is placed in the reading range of an RFID antenna. And Fig. 1(b) gives a 2D illustration from the top view. The initial position of the RFID tag is shown by a dashed line, and the state after flexing is indicated by a solid line. Let O denote the centroid of the tag, which coincides with the geometric center of the tag in an initial position. d and d' represent the antenna-tag distance before and after flexing. The tag orientation is measured by the absolute angle of $\angle O'OM$, *i.e.*, β . Table I shows the definitions of variables commonly used in this paper. The problem of tag flex-angle detection is formally defined as follows. *Flex-angle detection involves estimating the absolute angle of $\angle AOA'$, denoted as α , in the universal coordinate system. When a tag is flexed, its geometric center O remains unchanged, while the two ends A and B move towards A' and B' , respectively.*

B. RFlexor in a Nutshell

By analyzing the hardware characteristics of RFID tags, we propose an RFID-based Flex-sensor (RFlexor) to detect the flex-angle of an RFID tag.

Our system consists of three types of hardware devices: (i) an RFID reader with an antenna; (ii) a battery-free RFID tag; (iii) a backend server; and it includes three major blocks: data collection, calibration, and flex-angle detection. Specifically, To eliminate the interference of irrelevant parameters (*e.g.*, distance and orientation), we study the characteristics of the phase and RSSI models and leverage phase difference and RSSI ratio to derive a distance and orientation independent model. Finally, we use deep learning methods to perform regression on our pre-processed data and apply multi-head attention to assign weights to fuse phase and RSSI data, which enables the model to make use of the advantages of both types of measurements to achieve accurate flex-angle detection.

C. Challenges and Solutions

When implementing the RFlexor system, we need to address the following technical challenges.

The first challenge is how to refine the model in order to describe factors such as flexing. Previous RFID studies typically regards the tags as rigid items, and model the phase rotation and RSSI values as a function of antenna-tag distance. Thus, the traditional model cannot be used to derive the flexing angle of the target tag since the phase rotation and RSSI decay caused by the hardware circuit are usually regarded as constants during the flexing process. We have observed that the

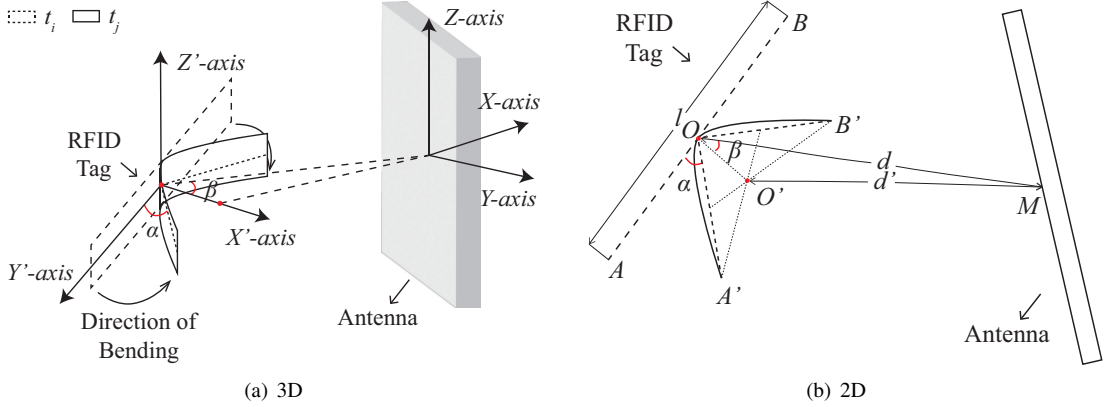


Fig. 1. Scene display of RFID tag's flex-angle detection

change in flexing angle affects the relative area and distance between circuits, and introduces additional phase rotations to the tag's circuit. Thus we reformulate phase and RSSI models by adding the factors of flexing angle, and orientation, which paves the way to derive the flex angles of tags from indefinite phase and RSSI measurements.

The second challenge is how to eliminate the effect of irrelevant orientation and distance parameters in the models. After obtaining the quantitative phase and RSSI models, we eliminate the effect of irrelevant parameters (e.g., orientation and distance), and derive the definite relationship between flexing angle and phase/RSSI data. Specifically, for a target tag with flexing angle $\alpha = a$, orientation angle $\beta = b$, and antenna-tag distance $d = x$, we need to pre-record the phase and RSSI data of the tag in its initial state (*i.e.*, $\alpha = 0$, $\beta = b$, $d = x$), and then compute the phase difference and RSSI ratio between flexing and initial states. Then, the interference of orientation and rotation can be eliminated, thereby having processed phase/RSSI data with a strong correlation with flexing angles.

The third challenge is how to adaptively fuse phase and RSSI to achieve accurate flex-angle detection. Although our empirical study shows that phase and RSSI are affected by tag flexing, how to derive the flexing angles from phase/RSSI data is still unknown. Since phase/RSSI data have different sensitivity to various environmental variations and interference factors, it is rational to adaptively fuse phase/RSSI data to utilize their strengths for better accuracy. We apply a multi-head attention model for capturing sequence patterns in different measurement sequences. Thus the model can automatically learn the hidden relationship between phase/RSSI data and flexing angles, and adaptively assign weights on these two data flows to archive accurate detection of tag flex-angles.

D. Novelty and Advantages

In this paper, we take the first step to enable batteryless flex-sensors via RFID tags and propose a system, called RFID-based Flex Sensor (RFlexor). The technical novelty of this paper lies in tackling three key challenges: (i) We refine the phase and RSSI model to describe the effects of flexing and

TABLE I
MAIN NOTATIONS USED IN THE PAPER.

Notations	Descriptions
θ	Phase value of target tag
θ_{reader}	Phase offset brought by RFID reader
θ_{flex}	Phase influence of tag flex-angle
θ_{orien}	Phase influence of tag-orientation
P_R	RSSI value received at RFID Reader
P_{flex}	RSSI influence of tag flex-angle
P_{orien}	RSSI influence of tag-orientation
α	Flex-angle of target tag
β	Orientation-angle of target tag
d_t	Distance between antenna and tag at time t
λ	RFID wavelength (default = 0.325m)

orientation by adding terms that specify flexing and orientation angles. (ii) We eliminate the effects of distance and orientation on flex-angle detection by collecting the phase and RSSI measurements from the same tags at the flexed state and initial states, respectively. By exploiting the difference between phase measurements and the ratio of phase measurements, the orientation- and distance-independent models can be obtained. (iii) We apply multi-head attention to automatically assign weights to the two data sources, thereby achieving better tag flex-angle detection. The advantages of RFlexor are two-fold: (i) Compared with the well-known flex sensor systems, our RFlexor system is battery-free and has an infinite lifetime; (ii) Compared with the computer vision systems, the proposed RFlexor system does not need a strong requirement on Line-of-Sight (LoS). We use the COTS RFID tags to implement the RFlexor system. Extensive experiment results show that RFlexor can achieve accurate flex-angle detection, *e.g.*, the detection error is less than 10 degrees with a probability higher than 90% at most conditions; and the average detection error is always less than 10 degrees across all experiments.

The remainder of this paper is organized as follows. We present the preliminary knowledge in Section II, and detailed system design in Section III. Section IV presents the implementation and the experimental results. We discuss the related work in Section V and conclude the paper in Section VI.

II. PRELIMINARY KNOWLEDGE

This section will present some preliminaries of the devices, data and basic mechanisms in RFlexor.

Typically, an RFID system consists of four major components: a reader, a scanning antenna, tags, and a data processing system. The reader uses radio waves to transmit signals that activate the tag. Once activated, the RFID tag sends a wave back to the antenna, where the energy and the vector changes of the wave is analysed. Specifically, the electromagnetic wave from the reader's scanning antenna induces a voltage on the tags, causing the tag to gain power and modulate its data onto the backscatter signal and then transmit it back to the reader. The reader can not only obtain a tag's EPC, but the low-level signal data that imply the spatial relationships between the tags and the reader: RF phase value, RSSI, and the received signal doppler value.

Phase: The RF phase value is a basic attribute of RF carrier waves that describe the degree to which the received signal is offset from the sent signal, ranging from 0 to 2π . Since a complete RFID signal transmission process is a round trip, the total distance traveled by the signal is $2d$. In addition to the RF phase rotation over distance, the tag's reflection characteristics, and the reader's receiver circuits will all introduce some additional phase rotation θ_{reader} and θ_{tag} , respectively. The total phase rotation can be expressed as:

$$\theta = \left[\frac{2d}{\lambda} \cdot 2\pi + \theta_{\text{reader}} + \theta_{\text{tag}} \right] \bmod 2\pi, \quad (1)$$

where λ is the wavelength and $\mu = \theta_{\text{reader}} + \theta_{\text{tag}}$ is determined by the hardware characteristics. Most commercial RFID readers (*e.g.*, as ImpinJ R420) are able to report θ as the difference between the transmitted and the received RF carriers, which reflects the distance d between the tag and the antenna. However, as the phase is a periodic value that repeats every λ in the distance of signal propagation, we cannot directly use these phase values to pinpoint deterministic tag locations.

RSSI: The power of the received radio signal is represented by RSSI, which has a negative logarithmic relationship with the distance between the tag and the reader. Specifically, the power of the signal received by an RFID reader can be expressed as:

$$P_R = P_T \frac{G_T G_R \lambda^2}{(4\pi d_0)^2}, \quad (2)$$

where d is the distance from the gravity center of the tag to the antenna, G_T and G_R are the gain of the transmitter and the receiver [4]. However, multipath propagation and undesired environmental interference can be combined with the primary backscatter, thereby increasing or decreasing the received signal power at the reader receiver.

III. SYSTEM DESIGN OF RFLEXOR

A. Observations and Insights

Observation 1: The phase and RSSI of an RFID tag are not only determined by the distance between the tag and the antenna, but also affected by the tag flexing angle.

We first re-investigate the standard phase model represented in Equation. (1) and RSSI model represented in Equation. (2), under flexing conditions. By fixing an RFID tag at a distance of 0.5m from the antenna, we recorded the phase and RSSI sequences at different angles of flexing (*i.e.*, 15°, 30°, 45°, 60° and 75°). We substitute the relevant parameters (*e.g.*, distance) into the equations, obtain the phase and RSSI values through AI models, and compare them with the corresponding collected data. Fig. 2 is an example of the phase and RSSI change. The figure on the left and right are the change of phase and RSSI, respectively. As the tag's flexing degree increases, its phase value gradually decreases, and the magnitude of the decrease becomes smaller. The difference is caused by the *flexing* of the tag. On one hand, The circuit of the RFID tag is commonly composed of a resistor and a capacitor in parallel. The impedance in the whole circuit will be affected as

$$Z = R + j(\omega L - \frac{1}{\omega C}) = R + j(\omega L - \frac{\epsilon s}{wd}), \quad (3)$$

where Z is the impedance, R is the resistance, C is the capacitance, ωL is the inductive reactance, $\frac{1}{\omega C}$ is the capacitive reactance, j is the imaginary unit, s is the facing area of the capacitor plate, and d is the distance of the capacitor plate. When the tag is flexing, its s and d will change dramatically, resulting in a change in the value of the capacitance in Equation. (3), which in turn affects the impedance of the entire circuit and ultimately affects the physical properties of the RFID tag. On the other hand, the antenna of the tag formalizes an equi-phase surface, according to which the tag can be equivalent to a point at the center of its collection. Therefore, the distance between the tag and the antenna is commonly considered as the distance from the center of the tag. However, when the tag is flexing, the surface would be interfered with, leading to various distances between the tag and the antenna. We add a parameter α to represent the flexing angle of the tag, thus the flexing offset of phase and RSSI can be written as $\theta_{\text{flex}}(\alpha)$ and $P_{\text{flex}}(\alpha)$. The mathematical models can be represented as

$$\theta = \left[\frac{2d}{\lambda} \cdot 2\pi + \theta_{\text{flexing}}(\alpha) + \theta_{\text{reader}} \right] \bmod 2\pi, \quad (4)$$

and

$$P_R = P_T \frac{G_T G_R \lambda^2}{(4\pi d_0)^2} P_{\text{flex}}(\theta). \quad (5)$$

Observation 2: For a flexing RFID tag under various tag orientations, the phase and RSSI would be different.

Under the same setup as above, we place the tag with a fixed flexing angle, then rotate it around point O by some degrees. The result is shown in Fig. 3, from which we can observe that. The phase model can be derived as [5]:

$$\begin{cases} \theta = (\frac{2\pi}{\lambda} \times 2d + \delta) \bmod 2\pi \\ \delta = \theta_0 + \theta_t + \theta_r \\ \tan \theta_0 = \frac{2(u \cdot w)(v \cdot w)}{(u \cdot w)^2 - (v \cdot w)^2}, \end{cases} \quad (6)$$

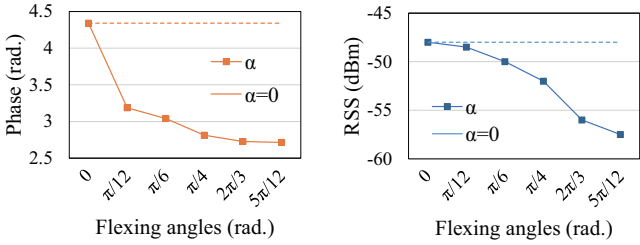


Fig. 2. Phase and RSSI change with different tag flex-angles

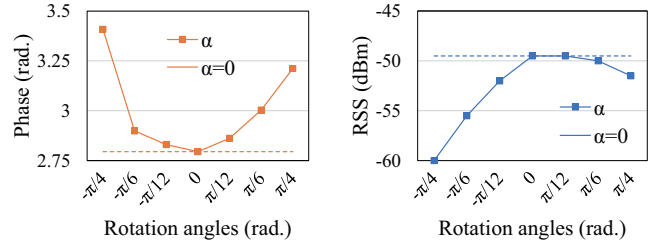


Fig. 3. Phase and RSSI change with different tag orientations

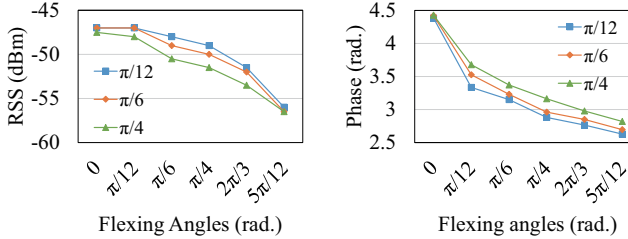


Fig. 4. Phase and RSSI range change with different tag-fex angles

where u , v , and w are the unit directional vectors of the reader antenna and the tag. Different from the traditional phase model in Equation. (1), the polarization-sensitive phase model explicitly takes into account the 3D orientation of the tag. However, in our work, the tag has a flexing angle, which makes the impact from flexing and orientation mixed up and can't be quantified. We add another parameter β to show the impact of orientation, the impacts on phase and RSSI are $P_{\text{orien}}(\beta)$ and $\theta_{\text{orien}}(\beta)$, respectively.

Hence, the Phase model and RSSI model in our work are built as follows:

$$\theta = \left[\frac{2d}{\lambda} \cdot 2\pi + \theta_{\text{flex}}(\alpha) + \theta_{\text{orien}}(\beta) + \theta_{\text{reader}} \right] \bmod 2\pi, \quad (7)$$

and

$$P_R = P_T \frac{G_T G_R \lambda^2}{(4\pi d_0)^2} P_{\text{flex}}(\alpha) P_{\text{orien}}(\beta). \quad (8)$$

By this, we split the unrepresentable θ_{tag} into quantities that are related to flexing α and orientation β . On the other hand, since these deforms and moves have no effect on the RFID reader, θ_{reader} is regarded as a constant. Hence, the phase and RSSI model have only three variables: α , β and d .

Observation 3: *The changing trend and range of phase and RSSI remain stable with different orientations and flexing angles of RFID tags.*

As shown in Fig. 4, our observations show that the phase/RSSI data is sensitive to the flexing changes but insensitive to the orientation changes. As shown in Fig. 4, when the tag is placed at different orientations, the overall offset caused by flexing and RSSI shifts slightly, but the change range remains nearly the same. e.g., the RSSI values change from -47dBm to -56dBm. Such trends will not change due to calibration (e.g., subtraction with the baseline), which paves

the way for flexing angle sensing using RSSI and phase data. This observation shows that the effect of rotation is not negligible but weak. In contrast, the effect of flexing is more pronounced. Which is the basis for our accurate measurement of the flexing angle.

B. System Overview

As shown in Fig. 5, RFlexor mainly consists of three parts: Data Collection, Calibration, and Flex-angle Detection. Firstly, in the block of data collection, we record RFID data and RSSI data. However, calibration is needed for dismissing the influence of other irrelevant factors (e.g., orientation, distance) on flexing sensing. Therefore, in addition to taking the data under a certain flexing state, we also need to collect the phase and RSSI of unflexed tag for reference. We study the characteristics of the phase and RSSI models respectively and find that in the phase model, most of the irrelevant factors can be eliminated by subtraction. While in the RSSI model, we can divide the data collected in the flexed state with the calibration data, thereby eliminating those factors. Through these operations, we obtain phase and RSSI models that are only affected by a few factors we care about, which can be directly fed into AI models. Finally, in AI model training, we estimate the flexing angle of a tag given the phase and RSSI data. We will elaborate on the technical details of the above building blocks in the following sections.

C. Details of RFlexor

1) Collecting Data: In this part, we introduce the data collection process in detail. The collection consists of two steps: The first step is to collect the phase and RSSI sequences from the tag in the initial state, and the second step is to collect the same type of information from the tag in the flexed state. In the first step, we set to collect the phase and RSSI sequence with a length of 200, which takes about 0.5 seconds. We leverage LLRP protocol to control the RFID reader can obtain phase and RSSI values via a single query command. In order to speed up the data collection process, we have set a filter in the program that allows us to filter tags based on the target ID by restricting the response of irrelevant tags. Thus, we get phase and RSSI sequences of the target tag, each of which contains 200 values collected in consecutive time frames. Then, in the second step, we flex the target angle, and then start to collect phase and RSSI sequences from the tag following the same settings as in the first step. To sum up,

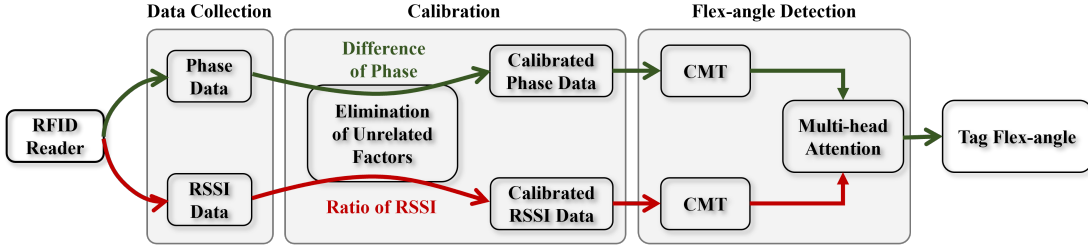


Fig. 5. Overview of the RFlexor system

after the data collection, we get a total of four sequences of length 200, two of which are phase, two are RSSI; two are unflexed, and two are flexed to the target angle. These four sequences are grouped according to phase and RSSI, and then will be used as two independent data sources to participate in the subsequent data processing and deep learning.

2) *Eliminating the Effects of Orientation and Distance:* We want RFlexor to be unaffected by factors other than flexing, thus we need to do some operations with the phase and RSSI models to get rid of those parameters that are not required. To reach this goal, we introduce the process of calibration, through which we can eliminate those factors. To be specific, under the condition that other conditions remain unchanged (*i.e.*, same distance, same orientation), we need to first collect the phase and RSSI of the tag in the unflexed state as a benchmark. In the case of constant environmental conditions, calibration is only required once. That is to say, after the calibration is completed, if we want to know any flexing angle of the tag, we can directly collect the phase and RSSI data of the tag at that position. As mentioned in Section III-A, the phase and RSSI models are only determined by flexing angle α , orientation angle β , and the distance d between the RFID tag and the antenna. Among them, the distance greatly affects the applicability of this model. In practical scenarios, it is difficult to control every flexing and rotation of the tag to be in the same position, or to measure the distance before every action. Therefore, it is necessary to remove the influence of different antenna-tag distances. To solve this, we optimize the signal propagation model reasonably and eliminate irrelevant variables to reduce interference.

Phase Model: Let 0 be the time for calibration and t be the time when the tag is at the target flexing angle, thus the phase at 0 and t are $\theta_{\text{flex}}(0)$ and $\theta_{\text{flex}}(t)$, respectively. According to (7), we can get the following equation.

$$\begin{aligned} \delta\theta &= \theta_0 - \theta_t \\ &= \left[\frac{2(d_0 - d_t)}{\lambda} \times 2\pi + \theta_{\text{flex}}(0) + \theta_{\text{orien}}(0) \right. \\ &\quad \left. - \theta_{\text{flex}}(t) - \theta_{\text{orien}}(t) \right] \mod 2\pi \quad (9) \\ &= \left[\frac{2\delta d}{\lambda} \times 2\pi + \theta_{\text{flex}}(0) - \theta_{\text{flex}}(t) \right] \mod 2\pi, \end{aligned}$$

where δd is the distance difference between time 0 and t , and it is much easier to obtain δd than d . Notably, we have noticed

that the distance between the tag and the antenna changes when the tag is flexing. That is, when a tag is flexing, we cannot regard its geometric center as its phase center, thus $\delta d \neq 0$. By taking the difference of the phase signals at two different locations, we transform the expression associated with the variable θ into $\delta\theta$. Because our intention is to estimate flexing angle using collect phase and RSSI data, we can rewrite Equation. (9) in another form with the flexing angle α_t at time t as the only independent variable:

$$\alpha_{t1} = F(\theta_{\text{flex}}(0), \theta_{\text{flex}}(t)). \quad (10)$$

So far, we have obtained a Function F . For the phase sequence at an arbitrary moment, we can estimate the corresponding flexing angle through F .

RSSI Model: On the RSSI side. Instead of subtraction, we divide the RSSI values at two different times 0 and t according to (8), and we can have the following equation.

$$\begin{aligned} \delta P_R &= \frac{P_{R_0}}{P_{R_t}} \\ &= \frac{P_T \frac{G_T G_R \lambda^2}{(4\pi d_0)^2} \cdot |P_{\text{flex}}(0)| \cdot |P_{\text{orien}}(0)|}{P_T \frac{G_T G_R \lambda^2}{(4\pi d_t)^2} \cdot |P_{\text{flex}}(t)| \cdot |P_{\text{orien}}(t)|} \\ &= \frac{d_0^2}{d_t^2} \cdot \frac{|P_{\text{flex}}(0)| \cdot |P_{\text{orien}}(0)|}{|P_{\text{flex}}(t)| \cdot |P_{\text{orien}}(t)|} \\ &= \frac{(d_0 + \delta d)^2}{d_0^2} \cdot \frac{|P_{\text{flex}}(0)| \cdot |P_{\text{orien}}(0)|}{|P_{\text{flex}}(t)| \cdot |P_{\text{orien}}(t)|}. \end{aligned}$$

Since δd is much smaller than d_0 , the equation can be further written as

$$\delta P_R \approx \frac{|P_{\text{flex}}(0)| \cdot |P_{\text{orien}}(0)|}{|P_{\text{flex}}(t)| \cdot |P_{\text{orien}}(t)|} = \frac{|P_{\text{flex}}(0)|}{|P_{\text{flex}}(t)|}. \quad (11)$$

Similarly, we can also convert the RSSI model into another function for the flexing angle α .

$$\alpha_{t2} = R(P_{\text{flex}}(0), P_{\text{flex}}(t)). \quad (12)$$

Hence, we have eliminated d in both phase and RSSI model, and can directly obtain the flexing angle α through given phase and RSSI data.

$$\begin{cases} \alpha_{t1} = F(\theta_{\text{flex}}(0), \theta_{\text{flex}}(t)) \\ \alpha_{t2} = R(P_{\text{flex}}(0), P_{\text{flex}}(t)) \\ \alpha_t = W(\alpha_{t1}, \alpha_{t2}), \end{cases} \quad (13)$$

where W is a weight function used to determine the respective status between phase and RSSI, while it is difficult to quantify. Deep learning essentially learns the relationship between

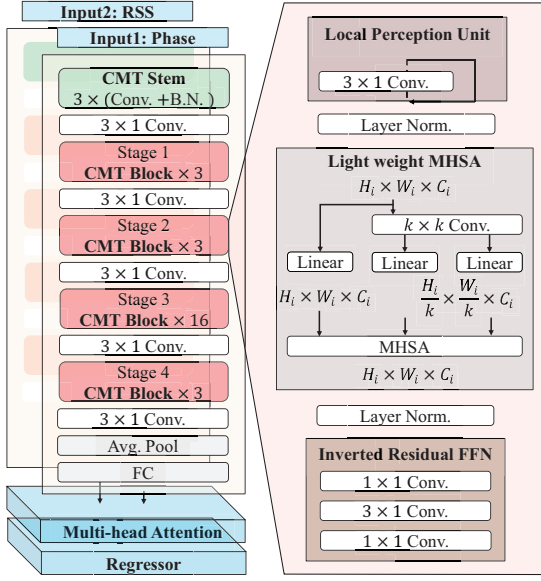


Fig. 6. Structure of network

variables, thus in this paper, we choose to use deep learning to quantify function F and R , and assign the weight between them.

3) *Detecting the Tag Flex-angle:* In this section, we introduce how to train the AI model in detail. For a sequence of phase and RSSI information at arbitrary antenna-to-tag distances and orientation angles, we would like to know how much its flexing angle is. In this paper, we refer to CMT [6], which consists of a new transformer based hybrid network, which is good at capturing long-range dependencies, and of CNNs to extract local information. Fig. 6 shows the detailed structure of the flexing regression model. Specifically, our network consists of a CMT stem layer, 4 CMT blocks, and a convolutional layer of convolution in the middle of each SMT block. We first need to acquire the phase and RSSI of the tag without flexing as initial state, and then after it is flexing, acquire its phase and RSSI sequence again. We make real-time phase sequence minus initial phase, and then divide each item in the RSSI sequence by initial RSSI. Finally, the obtained new sequence is passed into the model as the input of the model. Different from CMT, we change the original single image input of the network to the dual sequences input of phase and RSSI. We pass these two data into the network as two inputs, so that their respective characteristics can be better learned. Input data first go through the convolution stem for fine-grained feature extraction, and then is fed into a stack of CMT blocks for representation learning. Since data is constantly being in for training, the internal parameters of the network are constantly changing, resulting in inconsistent input distribution of each layer, which is called Internal Covariate Shift. To solve this, we add a batch normalization layer after each convolutional layer in the stem. Note that, the introduced CMT block is an improved variant of transformer block whose local information is enhanced by depth-wise convolution. The output of the model is the predicted flex-angle. We apply

a residual network to improve the depth of the network, because its internal residual blocks use skip connections, which can alleviate the network degradation problem caused by increasing depth in deep learning neural networks.

Impact of Tag Orientation Pattern: We notice that the changes in orientation lead to changes in phase thresholds. Specifically, when a tag is facing the antenna, we denote the range of phase change with flexing as $(\theta_{\min}, \theta_{\max})$. When the tag forms a certain rotation angle with the antenna, the range will change to $(\theta'_{\min}, \theta'_{\max})$, while its RSSI value is almost unchanged. The phase changes significantly but is greatly affected by the orientation angle, conversely, RSSI changes weakly but stable. To this end, we add a multi-head attention [7] layer before the residual network. The essence of the multi-head attention mechanism is to compute multiple attentions in parallel, connect their outputs, and provide them to the outputs through affine transformations to prevent overfitting. Since the weights themselves are functions of the input, the attention usually refers to computing convex combinations of content-based sequences of vectors. The mathematical definitions are as follows:

$$ATT_{Q,K,V} = \sum_i \alpha_i x_i, \quad (14)$$

where $\alpha_i = \text{softmax}\left(\frac{QK^T}{\sqrt{d_k}}\right)V$.

In this equation, x is the input series, q is the query factor, and $\sqrt{d_k}$ is the k -th dimension between a query and the key vector. Using attention rather than sentence pooling operators such as recurrent neural networks has many advantages, the most important of which is high computational efficiency in highly parallel environments.

IV. PERFORMANCE EVALUATION

In this section, we conduct experiments to evaluate the performance of RFlexor. We first describe the system implementation and the experiment settings. Then we conduct experiments to evaluate the performance of our system under various conditions and present the experimental results in three aspects: flexing sensing on various tags, at various rotation angles, and distances.

A. Implementation

As shown in Fig. 7, the hardware components of RFlexor system consist of an Impinj Speedway R420 reader, a Laird S9028PCR reader antenna, several Impinj E44 tags, and other two kinds of tags, embedded with Impinj Monza 4QT and NXP Ucode 8 chips. The data processing and training were carried out on a laptop, and a high-performance server DELL 7920 with an Nvidia Tesla P100 GPU, respectively. In terms of software components, we adopt the Octane Java SDK to develop a program running on the laptop to control the RFID reader to report Phase and RSSI data. We select a few points on the tag and attached them to toothpicks to control its flexing degree. Specifically, we insert small holes on the pre-marked angle disc in advance. When we need the tag to be fixed at a

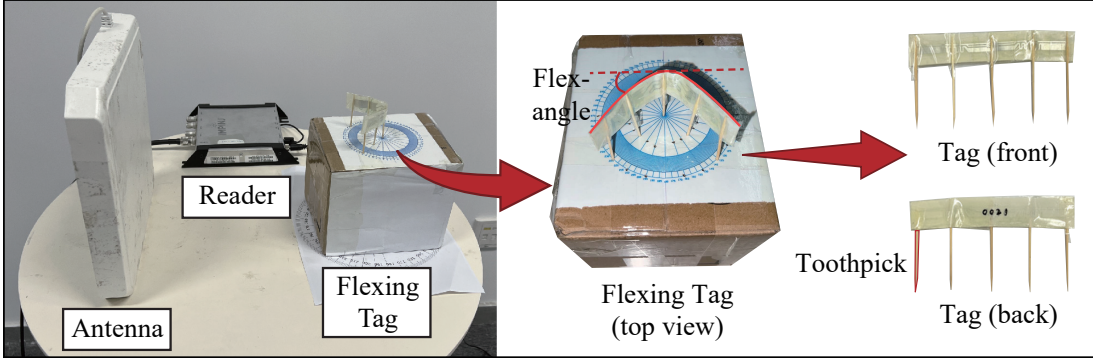


Fig. 7. Implementation of the proposed RFlexor system

particular flexing angle, we can directly insert the toothpicks into the holes of the corresponding angle, and thus the tag can stay still on that flexing angle.

B. Experiments

In the following, we show our detailed experiments and results. For training data, we collect 194 groups of data with orientation granularity of 15 degrees, that means we only collected data for 0, 15, 30, 45, 60, 75 and 90 degrees. However, in the test data, the flexing angle can be an arbitrary value in the range (0, 90). Our judging criterion is the difference between the predicted value and the actual flexing angle, and the absolute value of this difference is used as the error. We count the probability that the error is within 2.5° , 5° , 10° , 15° and 30° degrees respectively and use Cumulative Distribution Function (CDF) to show the experimental results since it can not only show the accuracy of the prediction but also fully describe the probability distribution of the prediction accuracy. We collected data at a distance of 30cm and 50cm for the training, in order to find features independent of distance. And we collect extra data at distances of 30cm, 50cm, and 70cm for testing. At each distance and orientation, we collect 40-100 groups of data to examine the robustness. Although the count of samples used in the model training is small, we utilize methods such as cross-validation in the network structure to prevent overfitting, and the robustness to other tags is presented in the experimental results.

1) *Impact of Tag Orientation:* We first verify whether we can sense the flexing angle accurately under various orientations between the tag and the antenna. The results upon -20° , 0 and 20° orientation angles are shown in Fig. 8, when the tag is facing the antenna (*i.e.*, $\beta = 0$), the probabilities that the error is within 2.5° , 5° , 10° , 15° and 30° are 41.18%, 70.59%, 94%, 100%. When $\beta = -20^\circ$, the probabilities are 46.67%, 80.00%, 100%, 100% and 100%. When $\beta = 20^\circ$, the probabilities are 43.75%, 62.51%, 100%, 100% and 100%. From the results with 15° orientation, RFlexor is able to achieve an accuracy of 100% within 7.5 degrees of error. It is notable that the training data is divided by 15 degrees, and the errors within 7.5 degrees are all regressed by the model's own training. In spite of we only show three orientation angles here, in fact,

RFlexor shows good results in each different orientation in our test results, the probabilities of the orientation angles of a is a . RFlexor can accurately perceive tag flex-angles with different tag orientations because we eliminate the amount related to β in phase and RSSI in the pre-processing stage. In this way, in the training data, the only variable is the flexing angle α , so different tag orientations will not affect the prediction of the model.

2) *Impact of Antenna-tag Distance:* In this set of experiments, we evaluate the influence of the distance between the RFID tag and the antenna. Since the typical effective sensing distance of RFID is about 2m, the experiments are set on the distance of 30cm, 50cm, and 70cm. Fig. 9 shows the results of the sensing accuracy on various distances. It can be found that the change in distance has no obvious impact on the sensing result. Specifically, since we want to verify the robustness of RFlexor upon distances, the training data consists of all data at 30cm and a little at 50cm, and the test data consists of the remaining 50cm data and all 70cm data. For the error of 15 degrees, the data at 30cm and 50cm reach the probabilities of 96% and 97%. On the other hand, we examine RFlexor on 100 groups of data collected at distance of 70cm. Even though our model has never seen 70cm's data, it predicts a probability of 100% within 15 degrees of error, which proves the robustness of the distance of RFlexor. As introduced in Section III, since we pre-process the phase and RSSI, the same part of the path of the tag under different flexing conditions is eliminated, that is, the distance between the antenna-tag and the phase is eliminated. This not only proves the distance-independent property of RFlexor, but also verifies the effectiveness of our distance elimination method.

3) *Impact of Tag Diversity:* We wonder whether RFlexor could still be robust under different tags. Although there will be offsets between the phase values and RSSI collected at different times, the difference between the phase and RSSI can still remain unchanged after calibration, and the data are then used for pattern identification. We first explore whether the sensing accuracy can be maintained between different RFID tags of the same type, and then further see whether the robustness can be maintained between tags of different types. We collect the phase and RSSI data of two other RFID tags of

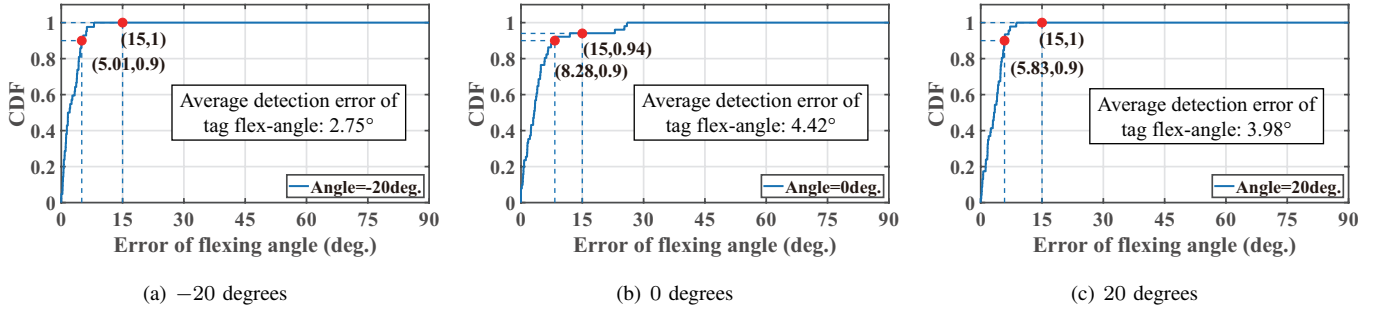


Fig. 8. Flex-angle detection results with different tag orientations

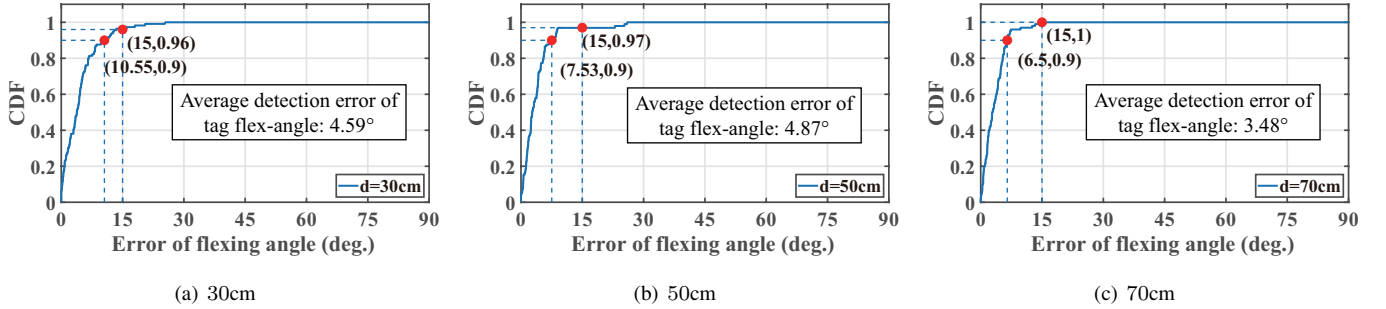


Fig. 9. Flex-angle detection results with different antenna-tag distances

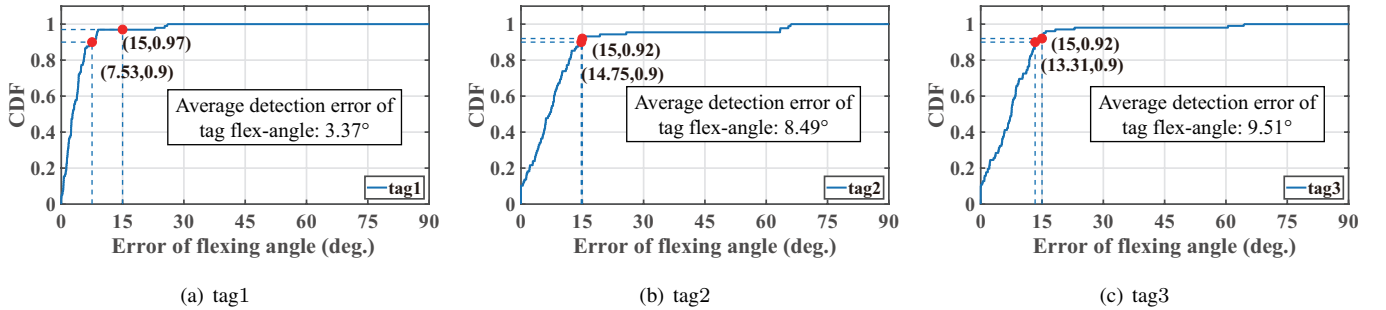


Fig. 10. Flex-angle detection results with different tags

the same pattern under different bending degrees and directly fed them into the model to observe the predicted results. Results in Fig. 10 show the RFlexor maintains robustness among RFID tags with the same pattern, where the collected data are all from tag 1, and the other two tags are only for testing. The three tags all reach a probability higher than 92%, with an error less than 10 degrees. This is because although the tags with the same pattern have different EPC IDs at their factory setting, but have similar hardware characteristics. Thus, it is normal for the tags with the same pattern to have similar performance on flexing sensing.

4) Impact of Relative Tag Positions: Finally, we want to show a whole picture of the flex-angle prediction result, which contains all conditions including orientations (*e.g.*, -30° , -20° , -10° , 0° , 10° , 20° , and 30°) and distances (*e.g.*, 30cm, 40cm and 50cm). From Fig. 11, flex sensing through RFlexor achieves an 8.12 degrees error of 90% data, and more than 97% of the data reaches a predicting error of not larger than

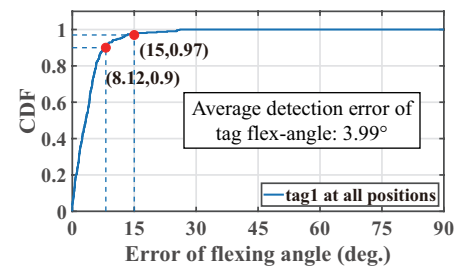


Fig. 11. Flex-angle detection results at different relative positions

15 degrees.

In this section of experiments, we first conducted experiments under three different conditions to prove that Flexor can still achieve good recognition accuracy under these conditions. Second, we combine these conditions to demonstrate that RFlexor can maintain high robustness in a complex environment where multiple influencing factors exist simultaneously.

Hence, based on the above experiments, we have demonstrated the high accuracy of RFlexor in identifying flexing angles, as well as the high robustness under different environmental conditions.

V. RELATED WORK

Through a thorough review of related works, we find no existing work exactly addresses the problem of tag flex angle detection. Hence, in what follows, we first discuss two categories of works that detect the physical states of RFID tags, including localization and pose estimation. Since this paper leverages tag hardware characteristics to detect tag flex angles, we also review the works that use tag hardware characteristics to enable sensing functionalities such as recognizing environmental temperature and humidity.

A. Localization and Tracking

Localization and tracking methods generally build mathematical models by exploiting the effect of distance on various kinds of data (*e.g.*, phase, RSSI). STPP [8] analyzes the vertex of phase profile to find the relative position of the tagged objects. RF-scanner [9] calculates tag positions by fitting to phase profile. MRL [10] and SILoc [11] calculate the position of the target tag in both 2D and 3D localization with the geometric relationship between the target tag and the antenna trajectory. SAH [12] proposes a phase-based localization method called Segment Aligned Hologram (SAH) that takes the unknown phase center (PC) and the phase offset (PO) fully into account. Speed Inconsistency-Immune approach to mobile RFID robot Localization (SILoc) [11] employs multiple antennas fixed on the mobile robot to collect the phase data of target tags, and can accurately locate RFID tagged targets when the robot moving speed varies or is even unknown. 3D-OmniTrack [13] is an approach that tracks the 3D location and orientation of an object and can achieve centimeter-level location accuracy with an average orientation error of 5 degrees. RED [14] tracks the position and polarization of the object through a polarization-sensitive phase model in an RFID system and uses the time and phase distribution of tag readings as effective features for eccentricity detection.

B. Pose Estimation

Tag-Compass [15] is a fine-grained direction recognition system that attaches a single tag to an object and identifies the tagged object's orientation by determining the spatial direction. Tagyro [16] proposes the first wireless sensing system that can track the 3D orientation of passive objects. RF-Kinect [17] treats the limbs of the human body as a whole. According to the body structure and the phase difference of the reference RFID tags, RF-Kinect achieves accurate body pose estimation. RF-Dial [18] tracks object translation and rotation using a fixed tag array topology by modeling the relationship between tag array phase changes and the object's rigid transformation. TIMU [19] develops an analytical model to capture the impact of polarization on the received signal and an optimization framework to incorporate the model to estimate the movement.

OmniTrack [5] proposes an orientation-aware phase model to explicitly quantify the respective impact of the read-tag distance and the tag's orientation. Spin-Antenna [20] builds a model to investigate RSSI and phase variation of RFID tags during antenna spinning and extends the model from a single tag to a tag array.

C. Target Sensing

GreenTag [21] attaches two RFID tags to a plant's container so that changes in soil moisture are reflected in their Differential Minimum Response Threshold (DMRT) metric at the reader. RIO [22] utilizes the impedance changing when a human finger touches the RFID tag to implement different interactions. RFIQ [23] and RF-EATS [24] use the tag's electromagnetic interactions with food or liquids in closed containers to detect their quality. Zannas *et al.* [25] leveraged changes in the antenna's impedance to sense temperature by utilizing the substrate's inherent properties to alter its complex impedance as temperature change. Tagtag [26] explores the use of RF signals for fine-grained material sensing with RFID devices and achieves high accuracy in identifying similar materials, like Pepsi and Coke. TagRay [27] is a contactless RFID-based sensing system, which significantly improves tracking accuracy, enabling mobile object tracking and even material identification. Wang *et al.* [28] utilized the intuition that varying degrees of RSSI reduction when tags penetrate different materials to simultaneously detect objects' material and shape. Chen *et al.* [29] designed the Thermotag and detected the temperature by measuring discharging period of the RFID tag. TwinLeak [30] is a liquid leakage detection system, which uses the inductive coupling effect between two adjacent tags as an effective feature for leakage detection.

VI. CONCLUSION

In this paper, we took the first step to enable batteryless flex-sensors via RFID tags, and the proposed system is called RFID-based Flex-sensor (RFlexor). Three key technical challenges were addressed when implementing the Rflexor system. First, under the challenging condition of adding flexing parameters to the mathematical models, we quantify and refine the function of the label's hardware characteristic. Second, to reduce the influence of irrelevant factors (*e.g.*, tag orientation, and antenna-tag distance), we proposed a calibration method to eliminate them from the equation. Third, we used multi-head attention in the AI model to intelligently assign weights to two data flows, rather than directly merging them together. Rflexor is implemented via COTS RFID devices. Extensive experiments demonstrate that fine-grained flex-angle detection results can be achieved, *e.g.*, the detection error of Rflexor is less than 10 degrees with a probability higher than 90% at most conditions, and the average detection error is always less than 10 degrees across all experiments.

ACKNOWLEDGMENT

This work is supported in part by the National Natural Science Foundation of China under Grant No. 62002259.

REFERENCES

- [1] J. H. Low, J. Goh, N. Cheng, P. Khin, Q. Han, and C.-H. Yeow, "A Bidirectional 3D-Printed Soft Pneumatic Actuator and Graphite-Based Flex Sensor for Versatile Grasping," in *Proc. of IEEE ICRA 2020*. IEEE, 2020, pp. 7979–7985.
- [2] T. J. Pannen, S. Puhlmann, and O. Brock, "A Low-Cost, Easy-to-Manufacture, Flexible, Multi-Taxel Tactile Sensor and its Application to In-Hand Object Recognition," in *IEEE ICRA 2022*, pp. 10939–10944.
- [3] S. H. Kim, H.-S. Chang, C.-H. Shih, N. K. Uppalapati, U. Halder, G. Krishnan, P. G. Mehta, and M. Gazzola, "A Physics-Informed, Vision-Based Method To Reconstruct All Deformation Modes in Slender Bodies," in *Proc. of IEEE ICRA 2022*, pp. 4810–4817.
- [4] K. Finkenzeller, *RFID Handbook: Fundamentals and Applications in Contactless Smart Cards, Radio Frequency Identification and Near-Field Communication*. John wiley & sons, 2010.
- [5] C. Jiang, Y. He, X. Zheng, and Y. Liu, "OmniTrack: Orientation-aware RFID Tracking with Centimeter-level Accuracy," *IEEE Transactions on Mobile Computing*, vol. 20, no. 2, pp. 634–646, 2019.
- [6] J. Guo, K. Han, H. Wu, Y. Tang, X. Chen, Y. Wang, and C. Xu, "CMT: Convolutional Neural Networks Meet Vision Transformers," in *Proc. of IEEE/CVF CVPR*, 2022, pp. 12175–12185.
- [7] A. Vaswani, N. Shazeer, N. Parmar, J. Uszkoreit, L. Jones, A. N. Gomez, Ł. Kaiser, and I. Polosukhin, "Attention is All You Need," in *Proc. of NIPS*, vol. 30, 2017.
- [8] L. Shangguan, Z. Yang, A. X. Liu, Z. Zhou, and Y. Liu, "STPP: Spatial-Temporal Phase Profiling-Based Method for Relative RFID Tag Localization," *IEEE/ACM Transactions on Networking*, vol. 25, no. 1, pp. 596–609, 2016.
- [9] J. Liu, F. Zhu, Y. Wang, X. Wang, Q. Pan, and L. Chen, "RF-Scanner: Shelf Scanning with Robot-assisted RFID Systems," in *Proc. of IEEE INFOCOM*, 2017, pp. 1–9.
- [10] X. Liu, J. Zhang, S. Jiang, Y. Yang, K. Li, J. Cao, and J. Liu, "Accurate Localization of Tagged Objects Using Mobile RFID-augmented Robots," *IEEE Transactions on Mobile Computing*, vol. 20, no. 4, pp. 1273–1284, 2021.
- [11] J. Zhang, X. Liu, T. Gu, X. Tong, S. Chen, and K. Li, "SILOC: A Speed Inconsistency-Immune Approach to Mobile RFID Robot Localization," in *Proc. of IEEE INFOCOM*. IEEE, 2021, pp. 1–10.
- [12] X. Zhang, J. Liu, X. Chen, W. Li, and L. Chen, "SAH: Fine-grained RFID Localization with Antenna Calibration," in *Proc. of IEEE INFOCOM*. IEEE, 2022, pp. 980–988.
- [13] C. Jiang, Y. He, S. Yang, J. Guo, and Y. Liu, "3D-OmniTrack: 3D Tracking with COTS RFID Systems," in *Proc. of ACM/IEEE IPSN*, 2019, pp. 25–36.
- [14] Y. He, Y. Zheng, M. Jin, S. Yang, X. Zheng, and Y. Liu, "Red: RFID-based Eccentricity Detection for High-speed Rotating Machinery," *IEEE Transactions on Mobile Computing*, vol. 20, no. 4, pp. 1590–1601, 2019.
- [15] J. Liu, M. Chen, S. Chen, Q. Pan, and L. Chen, "Tag-Compass: Determining the Spatial Direction of an Object with Small Dimensions," in *Proc. of IEEE INFOCOM*. IEEE, 2017, pp. 1–9.
- [16] T. Wei and X. Zhang, "Gyro in the Air: Tracking 3D Orientation of Batteryless Internet-of-Things," in *Proc. of ACM MobiCom*, 2016, pp. 55–68.
- [17] C. Wang, J. Liu, Y. Chen, L. Xie, H. B. Liu, and S. Lu, "RF-Kinect: A Wearable RFID-Based Approach Towards 3D Body Movement Tracking," *Proceedings of the ACM on Interactive, Mobile, Wearable and Ubiquitous Technologies*, vol. 2, no. 1, pp. 1–28, 2018.
- [18] Y. Bu, L. Xie, Y. Gong, C. Wang, L. Yang, J. Liu, and S. Lu, "RF-Dial: An RFID-based 2D Human-computer Interaction via Tag Array," in *Proc. of IEEE INFOCOM 2018*, pp. 837–845.
- [19] S. Pradhan, S. Li, and L. Qiu, "Rotation Sensing Using Passive RFID Tags," in *Proc. of ACM MobiHoc*, 2021, pp. 71–80.
- [20] C. Wang, L. Xie, K. Zhang, W. Wang, Y. Bu, and S. Lu, "Spin-Antenna: 3D Motion Tracking for Tag Array Labeled Objects via Spinning Antenna," in *Proc. of IEEE INFOCOM*. IEEE, 2019, pp. 1–9.
- [21] J. Wang, L. Chang, S. Aggarwal, O. Abari, and S. Keshav, "Soil Moisture Sensing with Commodity RFID Systems," in *Proc. of ACM MobiSys*, 2020, pp. 273–285.
- [22] S. Pradhan, E. Chai, K. Sundaresan, L. Qiu, M. A. Khojastepour, and S. Ranganajan, "RIO: A Pervasive RFID-Based Touch Gesture Interface," in *Proc. of ACM MobiCom 2017*, pp. 261–274.
- [23] U. Ha, Y. Ma, Z. Zhong, T.-M. Hsu, and F. Adib, "Learning Food Quality and Safety from Wireless Stickers," in *Proc. of ACM HotNets*, 2018, pp. 106–112.
- [24] U. Ha, J. Leng, A. Khaddaj, and F. Adib, "Food and Liquid Sensing in Practical Environments using {RFIDs},," in *Proc. of USENIX NSDI 2020*, pp. 1083–1100.
- [25] K. Zannas, H. El Matbouly, Y. Duroc, and S. Tedjini, "Self-tuning RFID Tag: A New Approach for Temperature Sensing," *IEEE Transactions on Microwave Theory and Techniques*, vol. 66, no. 12, pp. 5885–5893, 2018.
- [26] B. Xie, J. Xiong, X. Chen, E. Chai, L. Li, Z. Tang, and D. Fang, "Tagtag: material Sensing with Commodity RFID," in *Proc. of ACM SenSys*, 2019, pp. 338–350.
- [27] Z. Chen, P. Yang, J. Xiong, Y. Feng, and X.-Y. Li, "Tagray: Contactless Sensing and Tracking of Mobile Objects using COTS RFID Devices," in *Proc. of IEEE INFOCOM*. IEEE, 2020, pp. 307–316.
- [28] J. Wang, J. Xiong, X. Chen, H. Jiang, R. K. Balan, and D. Fang, "Simultaneous Material Identification and Target Imaging with Commodity RFID Devices," *IEEE Transactions on Mobile Computing*, vol. 20, no. 2, pp. 739–753, 2019.
- [29] X. Chen, J. Liu, F. Xiao, S. Chen, and L. Chen, "Thermotag: Item-Level Temperature Sensing With a Passive RFID Tag," in *Proc. of ACM MobiSys 2021*, pp. 163–174.
- [30] J. Guo, T. Wang, Y. He, M. Jin, C. Jiang, and Y. Liu, "TwinLeak: RFID-based Liquid Leakage Detection in Industrial Environments," in *Proc. of IEEE INFOCOM*, 2019, pp. 883–891.